Effects of Thrust Noise on Drag-Free and Attitude Control System

IEPC-2019-343

Presented at the 36th International Electric Propulsion Conference
University of Vienna • Vienna, Austria
September 15-20, 2019

Kai Cui[1], Hui Liu[2], Wen-Jia Jiang[3] and Da-Ren Yu[4]
Harbin Institute of Technology, Harbin, Heilongjiang, 150001, China

Abstract: For space precision measurement tasks, the drag-free and attitude control system is the key technology to minimize disturbances of space environment to scientific measuring instruments and achieve stable flight of the satellite platform. But the thruster, as the actuator of the whole system, its noise characteristics also have particularly pernicious effects on the accuracy of the control system. In order to clarify the influence of thrust noise on the drag-free and attitude control system, thrust noise in millihertz band of a cusped field thruster is measured at first. Then, a drag-free and attitude control system is established. Finally, the effects of thrust noise in different frequency bands on control system are simulated and analyzed.

Nomenclature

a_d, a_T	=	accelerations of atmospheric drag and thrust
C_D	=	drag coefficient
e	=	elementary charge
f	=	thruster model
F_d	=	atmospheric drag
g	=	gravity function
I_i	=	ion current
i_o, j_o, k_o	=	three axes of local orbital reference frame
J	=	inertia tensor of the satellite
k_{pa}, k_{da}	=	control parameters of attitude control loop
k_{pdf}, k_{ddf}	=	control parameters of drag-free control loop
L_d	=	force arm of atmospheric drag
m	=	mass of satellite
m_i	=	atomic mass of Xenon
$\dot{m}_\iota$	=	anode flow rate
ρ_D	=	atmospheric density
q	=	attitude quaternion
r_s, r_t	=	position of satellite and test mass
δr	=	displacement error between satellite and test mass
S_D	=	frontal area of the satellite
T	=	thrust

[1] PhD student, Laboratory of Plasma Propulsion, and cuikai1313@gmail.com.
[2] Associate professor, Laboratory of Plasma Propulsion, and huiliu@hit.edu.cn.
[3] PhD student, Laboratory of Plasma Propulsion, and yyxc1993@163.com.
[4] Professor, Laboratory of Plasma Propulsion, and yudaren@hit.edu.cn.

τ_d, τ_a	=	torques of drag and actuator
U_a	=	anode voltage
U_i	=	accelerating voltage
v_{rel}	=	relative velocity of satellite and air
v_s, v_t, v_i	=	velocity of satellite, test mass and ion
$\omega, \hat{\omega}$	=	angular rate

I.Introduction

FOR space precision measurement tasks, high demands on the stability of the experimental environment are put forward to ensure the correct measurement of scientific signals. Taking the Gravity and steady state Ocean Circulation Explorer (GOCE) as an example, GOCE is a gravity satellite based on gravity gradiometer, which was successfully launched on March 17, 2009 by European Space Agency to determine the Earth's steady state gravity field anomalies with an accuracy of 1 x 10^{-5} m/s^2 and determine geoid heights with accuracy between 1 to 2 cm, at length scales down to 100 km.[1] In order to improve the accuracy of gravity field measurement, the orbit altitude of GOCE satellite is 250 km, but the fluctuation of atmospheric drag in near-earth orbit is large, which requires that the gravity gradiometer has a large dynamic measurement range.[2] However, the large measurement range inevitably leads to the decrease of the measurement resolution of the instrument. So, to improve the resolution of the gravity gradiometer and meet the stability requirements of GOCE, which requires the residual linear acceleration of the satellite to better than 2.3 x 10^{-8} ms^{-2}/√Hz[1], GOCE use the drag-free and attitude control system (DFACS) and electric thrusters to offset the non-conservative force in real time and minimize residual acceleration of the satellite platform.[3,4,5] In addition to gravity field missions, there are other space precision scientific measurement tasks that also use drag-free satellites, such as MicroSCOPE[6] (launched on April 25, 2016 from Kourou) for equivalence principle testing and LISA pathfinder[7] (launched on December 2, 2015) for gravitational wave detection technology testing.

There exists a free-falling test mass in a drag-free satellite. The goal of DFACS is making the satellite follow test mass as it falls through space affected only by gravity.[8] The principle of DFACS is to use the thrust of the thruster to compensate the non-conservative force of the space environment on the satellite in real time.[9]

The thruster, as the actuator of DFACS, its working performance seriously affects the control performance of the whole system, especially the thrust noise characteristics. Therefore, each task has a clear requirement for thrust noise in mHz-Hz band, for example, the thrust noise requirement of GOCE satellite is 0.05mN/√Hz in the measurement bandwidth.[10] The noise characteristics of a T5 Kaufman-type ion thruster were verified to meet the requirements of GOCE satellite and it was used in this satellite.[11] In order to design better controllers, some researchers have taken thrust noise into account when designing DFACS controllers[12,13], but it is still unclear how thrust noise affects the whole system. And the distribution of plasma oscillation spectrum is very wide[14], in which breathing mode instability (kHz band) plays a major role in the process of ionization, diffusion and acceleration of particles[15]. It is not known whether the oscillation in this higher frequency band could affect the accuracy of DFACS.

Therefore, the main research content of this paper is to analyze the influence of thrust noise in different frequency bands on the DFACS. The noise characteristics of a thruster are measured and analyzed firstly in Section II. Then a DFACS considering thrust noise is modeled in Section III. In Section IV, the effects of thrust noise in different frequency bands on the DFACS are presented and analyzed.

II.Thrust Noise of a Cusped Field Thruster

A cusped field thruster designed for drag-free satellites was tested in Plasma Propulsion Laboratory of Harbin Institute of Technology.[16] The previous experiments have proved that the thruster has the ability to be applied to drag-free satellites.[17] In this study, we mainly measure the thrust noise of this thruster under different operating conditions.

In GOCE mission, the science measurement bandwidth is 5 to 100 mHz. Therefore, the measurement bandwidth of thrust noise is set as 1mHz to 10Hz. However, due to the response speed limitation of the thrust stand, it is impossible to use the thrust stand to measure thrust above Hz band. So an indirect thrust measurement method is used, which calculates thrust by measuring plume parameters. Since thrust is generated by accelerated ions, thrust *T* can be theoretically expressed in the following formula:

$$T = \dot{m}_i v_i \tag{1}$$

where $\dot{m}_i$ is the anode flow rate, v_i is the ion velocity. According to the law of conservation of energy and conservation of mass,

$$v_i = \sqrt{2U_i\, e/m_i} \tag{2}$$

$$\dot{m}_\iota = I_i\, m_i/e \tag{3}$$

where U_i is the accelerating voltage, I_i is the ion current, and m_i, e represent atomic mass and elementary charge constant. Among them, the ion current in plume region can be measured by Faraday probe. RPA probe is used to measure ion energy distribution, which is accelerating voltage U_i, and two sets of data are combined to calculate the thrust value. The detailed calculation method of thrust is introduced in A. Keller's doctoral thesis[18], so it is not described in this section.

Thrust noises of this thruster under different operating conditions are measured. Among them, thrust noises of four conditions (Anode voltage U_a is 600V and 650V, anode flow rate $\dot{m}_\iota$ is 4sccm and 7sccm, respectively) are shown in Fig.1. According to the measured results, the thrust noise spectrum characteristics are basically the same under different operating conditions. And thrust noises under all working conditions meet GOCE thrust noise requirement (see the red thick line in the Fig.1).

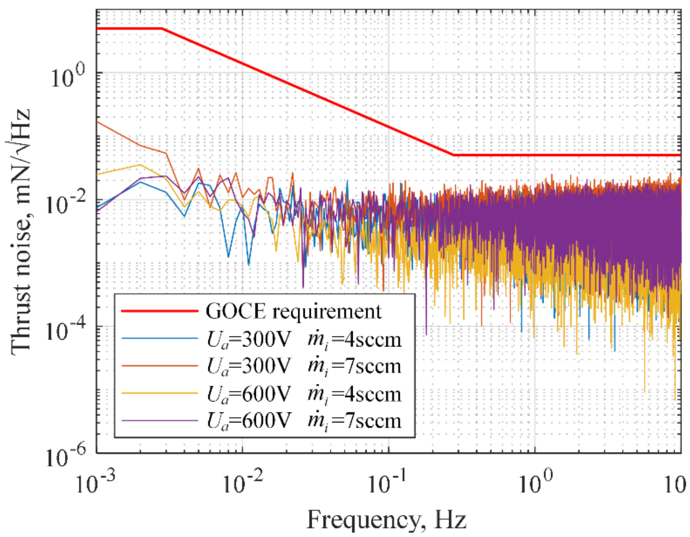

Figure 1. Amplitude spectral densities of thrust under four operating conditions

According to Fig. 1, the thrust noises have white noise characteristics that the amplitude spectral densities of thrust are evenly distributed in the frequency band above 0.05 Hz. This feature reflects the randomness of the system motion, which may be caused by random fluctuations of the input devices of the thruster (such as fluctuations of Xenon Feed Assembly) or plasma oscillations. Below 0.05Hz, thrust noise amplitudes increase slightly with decreasing frequency. Compared with the other three working conditions, the thrust noise increases obviously when the anode voltage equals 300V and anode flow rate is 7sccm. Therefore, thrust noise in this frequency band is specific and may be related to the long-term thermal drift of the thruster. The detailed reasons need to be further studied later.

III.Drag-Free and Attitude Control System Modeling

To analyze the effects of thrust noise on DFACS, the modeling method of DFACS is described in this section. The control block diagram of DFACS is shown in Fig. 2. The test mass is in free fall. There is a capacitive sensor to measure the displacement and velocity differences between the test mass and the satellite in real time. The displacement and velocity errors are delivered to the controller to generate thrust commands[19]. And thrust noise is considered when the thrust is calculated in the thruster model.

The goal of attitude control loop is to make the satellite attitude follows the local orbital reference frame (LORF) in real time. The axes in LORF are defined by[10]

$$i_o = \frac{v_s}{|v_s|},\ j_o = \frac{v_s \times r_s}{|v_s \times r_s|},\ k_o = j_o \times i_o \tag{4}$$

that means i_o points toward motion direction, j_o is aligned with the angular momentum direction. Because the main research content of this paper is to analyze the impacts of thrust noise on the whole system, it is assumed that the sensors and actuators in the attitude control loop are ideal devices without any noise.

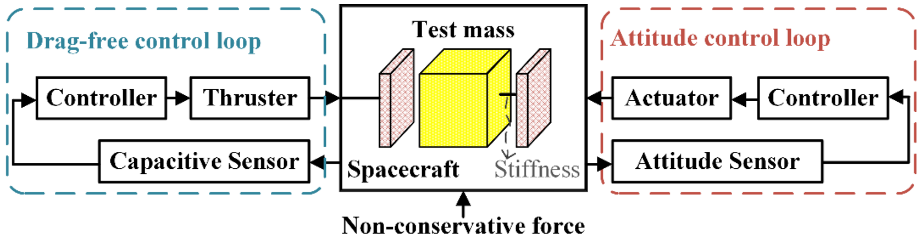

Figure 2. The control block diagram of DFACS

A. Orbital and attitude state equations

The test mass is in free fall and its motion is determined only by gravity. Therefore, its motion equation is

$$\dot{r}_t = v_t,\ \dot{v}_t = g(r_t) \tag{5}$$

where g is the gravity acceleration, which is a function of the position of test mass. Satellite motion is also affected by atmospheric drag and thrust, as shown in Eq. (6).

$$\dot{r}_s = v_s,\ \dot{v}_s = g(r_s) + a_d + a_T \tag{6}$$

where a_d is the accelerations of atmospheric drag and a_T represents thrust accelerations. For satellite attitude dynamics, Euler's equations and kinematic equations[20] based on quaternion are used,

$$\dot{q} = \frac{1}{2}\widehat{\omega} \cdot q \tag{7}$$

$$\dot{\omega} = J^{-1} \cdot [\tau_d + \tau_a - \omega \times (J \cdot \omega)] \tag{8}$$

where q is the attitude quaternion describing the attitude of the satellite, $\widehat{\omega}$ is the quaternion representation of the angular rate with regard to LORF, and J is inertia tensor (from GOCE). τ_d, τ_a are the torques of drag and actuator. With these equations, motion states of test mass and satellite can be calculated.

B. Environment forces and torques

Because the orbital altitude is 250 km, the atmospheric drag effect is very obvious, and the solar pressure can be neglected in the low Earth orbit. The atmospheric drag F_d is a function of a drag coefficient C_D, the frontal area of the satellite S_D, the atmospheric density ρ_D, and the relative velocity v_{rel}. Atmospheric drag acceleration a_d equals atmospheric drag divided by satellite mass m. The disturbance torque τ_d is equal to the force arm L_d multiplied by the drag value (see Eq. (10)). In this simulation, C_D is set as 2.2 and the atmospheric density ρ_D is calculated by the U.S. Naval Research Laboratory mass spectrometer and incoherent scatter radar model NRLMSISE-00.[21]

$$F_d = -\frac{1}{2} \cdot C_D \cdot S_D \cdot \rho_D \cdot v_{rel} \cdot |v_{rel}|, \qquad a_d = F_d/m \tag{9}$$

$$\tau_d = L_d \times F_d \tag{10}$$

C. Controller

For drag-free control loop, the displacement errors δr and velocity errors $\delta\dot{r}$ between satellite and test mass can be used as feedback signals. Based on the principle of proportional and differential control[22], the control law is shown in Eq. (11), where k_{pdf}, k_{ddf} are control parameters. Similarly, the controller of attitude control loop is shown in Eq. (12), k_{pa}, k_{da} are control parameters of this loop.

$$a_T = -k_{pdf} \cdot \delta r - k_{ddf} \cdot \delta \dot{r} + g(r_t) - g(r_s) - a_d \tag{11}$$

$$\tau_a = -k_{pa} \cdot q - k_{da} \cdot \omega - \tau_d \tag{12}$$

D. Thruster model considering thrust noise

At present, most of the researches on electric thrusters are concerned with the physical phenomena and high-frequency motion process of internal plasma. Thrusters are simulated mostly based on fluid method or Particle in Cell (PIC) method, but these methods are too computational and unsuitable for satellite control simulation. Because the control simulation step is 0.1s, the plasma dynamics can be neglected. Therefore, for this study, the thruster can be simplified as a simple multi-input and multi-out system (MIMO) without concern for the plasma motion inside the thruster. Anode flow rate and anode voltage are input parameters and thrust is output parameter of this system. The input-output model is established based on steady-state experimental data[17], which can be expressed as follows

$$T = f(\dot{m}_\iota,\ Ua) \tag{13}$$

In order to reflect the influence of thrust noise, the real thrust output value is equal to T plus thrust noise. Thrust noise is calculated based on experimental data. The amplitude spectral density of thrust noise can be obtained in Section 2. Random phase is artificially introduced to restore the noise signal.

IV.Simulation Results and Analysis

In this program, the orbital altitude is set at 250 km, eccentricity is 0.001 and the mass of satellite is 1052 kg, which are consistent with those of GOCE. To analyze the influence of thrust noise on the DFACS, we calculate the simulation without thrust noise firstly. Then we assume this cusped field thruster is used to compensate the along-track non-conservative forces, that means the thrust noise in i_o direction is considered in the second simulation.

The total simulation time of DFACS is 10000s. The simulation results of thrust and air drag in time domain are shown in the Fig. 3. From Fig. 3 a), it can be seen that the output thrust of the thruster can compensate the atmospheric drag in real time during the operation of the satellite, which shows the correctness of the simulation program and the controller design. Considering the thrust noise, the amplitudes of thrust output fluctuation increase dramatically (see Fig.3 b)). Although it can still compensate the atmospheric drag in real time, the errors of drag compensation increase obviously. Comparing two figures, the average error of drag compensation increases from 2.229μN to 48.210μN due to thrust noise.

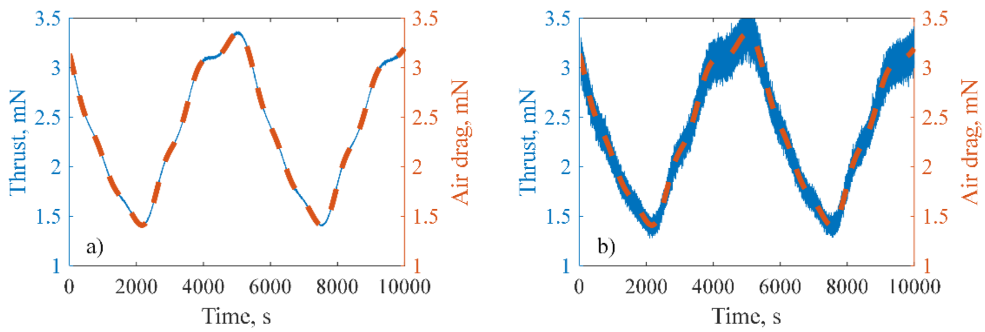

Figure 3. Thrust and air drag values in i_o axis, a) without noise, b) with noise

To further observe the effects of thrust noise on the drag-free control loop, the amplitude spectral densities of displacement and velocity errors between satellites and the test mass in three axes are given (as shown in the Fig. 4). These parameters can characterize the control performance of this control loop. Considering thrust noise only in the i_o direction, we can see that both displacement errors and velocity errors in this direction have great increases. The maximum displacement error increases from 3.453 nm to 87.155 nm, and the maximum velocity error reaches 72.867 nm/s from 3.256 nm/s. In j_o and k_o direction, the displacement errors and velocity errors increase slightly, the errors of thrust and air drag are also very small, and the control accuracy is basically unchanged. The results show that the thruster, as an actuator in the drag-free control loop, its noise directly affects the accuracy of drag compensation, which leads to the increase of the residual linear acceleration of the satellite and the decrease of the control precision. Therefore, thrust noise deteriorates the performance of the control system.

For the attitude control loop, the simulation results are shown in the Fig. 5. It can be seen that for the two cases, the amplitude spectral densities of attitude errors and attitude rates are basically the same, so the effects of thrust noise on the performance of attitude system can be neglected. This is because we assume that the thrust is directly acting on the center of mass of the satellite in this program, and its behavior does not cause significant changes in the attitude of the satellite, the simulation results are consistent with the current assumption. However, the thrust misalignment is inevitable in the actual operation process of the thruster, because of installation error of the thruster or the non-axisymmetric thrust output of the thruster. Therefore, when the thrust misalignment is taken into account, the thrust noise inevitably is coupled to the attitude control loop and produces disturbance torques, which affects the attitude control accuracy. Therefore, thrust noise has huge effects on the control accuracy of DFACS.

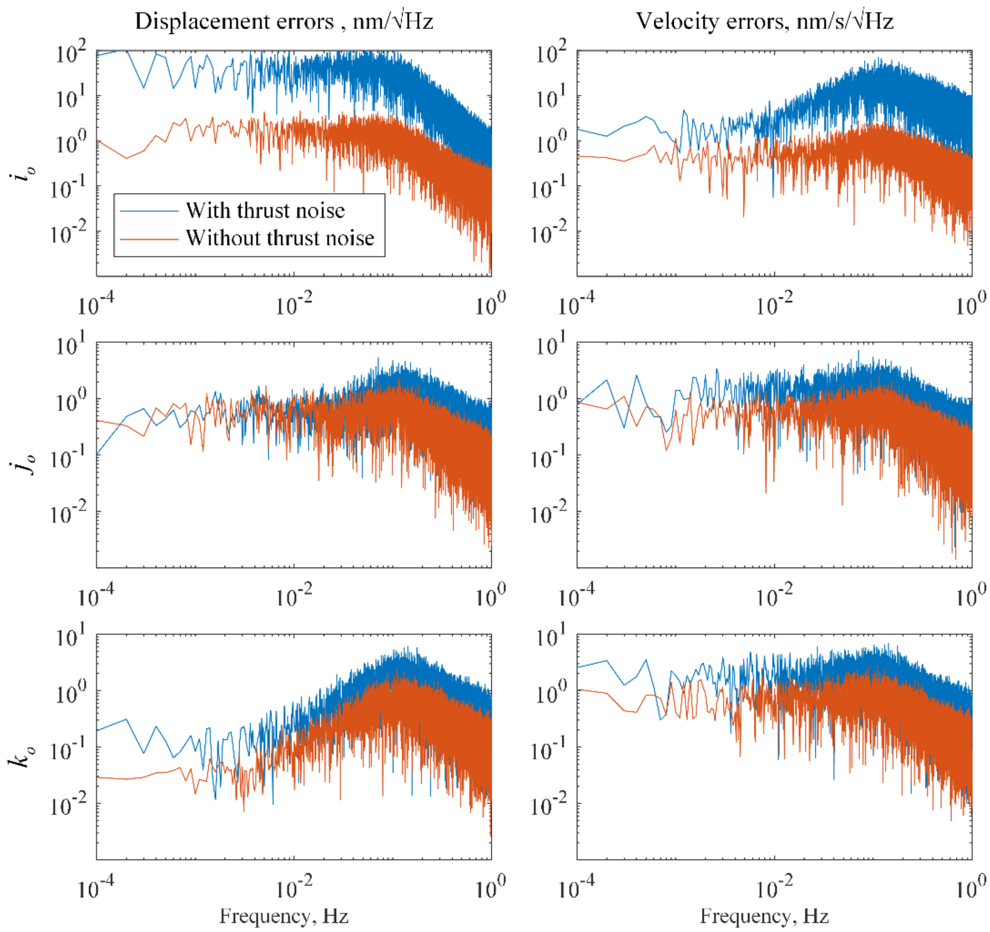

Figure 4. Displacement and velocity errors of drag-free control loop in three axes

Above all, the influence of thrust noise in mHz-Hz band on DFACS is analyzed. But according to the studies of electric thrusters, due to the movement of plasma and neutral gas, the frequency spectrum of discharge current oscillation covers kHz to GHz, and the amplitude of breathing oscillation (in kHz frequency band) is the largest, which has the most serious impacts on the thruster discharge and propulsion system. Therefore, the effects of higher frequency thrust noise on DFACS are simulated and analyzed next. Currently, there are many studies about breathing oscillation, and its formation mechanism has been understood. However, due to the difficulty and complexity of high-frequency measurement of thrust, the current research is basically centered on the discharge current, there is very little research on the thrust oscillation at kHz frequency band. Therefore, in this study, a sinusoidal wave with a frequency of 1 kHz and an oscillation amplitude of 10% is used to simulate the breathing oscillation of thrust, which is brought into the program for simulation calculation. Because of the huge amount of calculation, the simulation time is set to 100s.

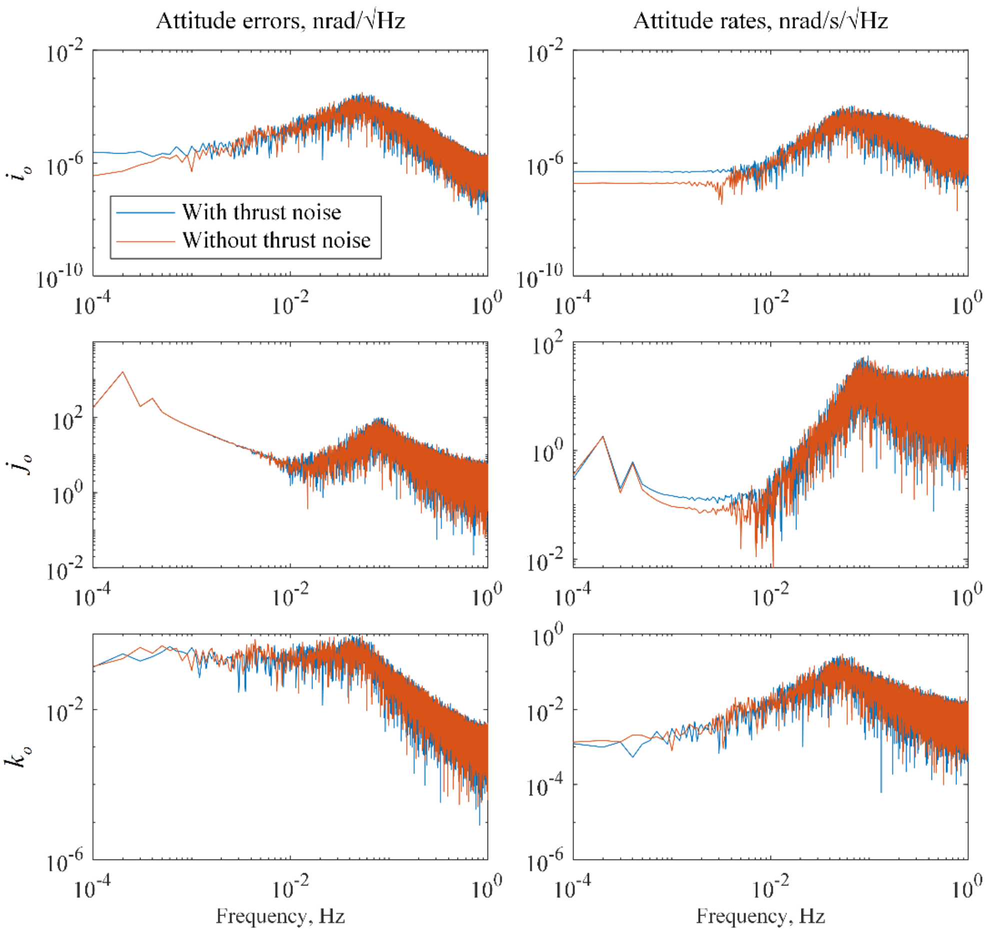

Figure 5. Attitude errors and attitude rates of attitude control loop in three axes

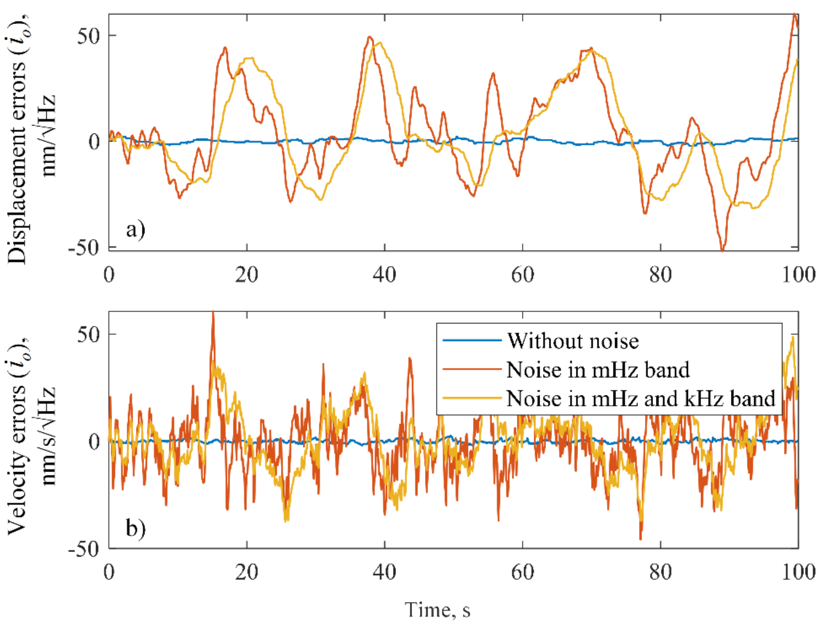

Figure 6. Displacement and velocity errors of drag-free control loop in i_o axis

Figure. 6 shows the simulation results of the displacement and velocity errors in i_o direction of three cases. Case 1 uses ideal thruster without thrust noise and case 2 considers thrust noise only in mHz band. The thrust noise in mHz and kHz band are considered at the same time in case 3. Figure. 7 shows the corresponding amplitude spectral densities of those parameters. It can be seen from the two graphs that although thrust noise in kHz band has slight effects on the control errors of drag-free control loop, the amplitude changes are not obvious. This is because satellite is a large inertial system, which can filter high frequency noise. Due to the limitation of system bandwidth, the influence of high-frequency thrust noise on DFACS can be neglected. In summary, the thrust noise in the scientific measurement frequency band (mHz-Hz) has significant impacts on DFACS, and the thrust fluctuation in higher frequency band need not be considered.

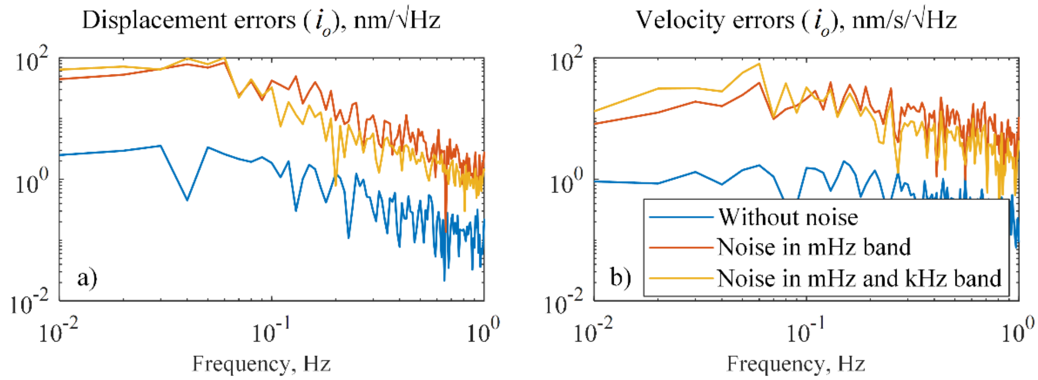

Figure 7. Amplitude spectral densities of displacement and velocity errors in i_o axis

V.Conclusion

The drag-free and attitude control system is a necessary means to realize the ultra-stable flight of a satellite and a necessary technology for space precision measurement experiments. As the actuator of drag-free control system, the output noise of a thruster affects the accuracy of the control system. In order to accurately analyze the impacts of thrust noise on the system, the thrust noise of a cusped field thruster is measured firstly. Then a drag-free satellite simulation system based on orbit mechanics, attitude dynamics, feedback control and thruster model is built. According to the simulation results, it is found that thrust noise directly affects the accuracy of drag compensation, and leads to significant increases in the displacement errors and velocity errors between the satellite and the test mass. For attitude control system, thrust noise has no obvious effects on it based on the current assumption. The influence of thrust noise in higher frequency band, such as breathing oscillation band, on DFACS can be neglected.

Therefore, the thrust noise and output stability of the thruster in mHz-Hz frequency band need to be further optimized to further reduce the effects of the thruster on the control accuracy of the DFACS.

Acknowledgments

The authors would like to acknowledge the National Natural Science Foundation of China (Grant Nos. 51776047 and 51736003).

References

[1]Allasio, A., Anselmi, A., Catastini, G., Cesare, S., Dumontel, M., Saponara, M., Sechi, G., Tramutola, A., Vinai, B., André, G., Fehringer, M., and Muzi, D. "Goce Mission: Design Phases and in-Flight Experiences." Advances in the Astronautical Sciences, Vol. 137, No. March 2014, 2010, pp. 627–646.

[2]Nguyen, A. N., and Conklin, J. W. "Three-Axis Drag-Free Control and Drag Force Recovery of a Single-Thruster Small Satellite." Journal of Spacecraft and Rockets, Vol. 52, No. 6, 2015, pp. 1640–1650. doi:10.2514/1.A33190.

[3]Canuto, E., Bona, B., Calafiore, G., and Indri, M. Drag Free Control for the European Satellite GOCE. Part I: Modelling. No. 2, 2002, pp. 1269–1274.

[4]Canuto, E., Molano, A., and Massotti, L. "Drag-Free Control of the GOCE Satellite: Noise and Observer Design." IEEE Transactions on Control Systems Technology, Vol. 18, No. 2, 2010, pp. 501–509. doi:10.1109/TCST.2009.2020169.

[5]Electric, I., Conference, P., and Park, C. T. Thrust Control Algorithms for the GOCE Ion Propulsion Assembly. 2007.

[6]Delavault, S., Prieur, P., Liénart, T., Robert, A., and Guidotti, P. Y. "MICROSCOPE Mission: Drag-Free and Attitude Control System Expertise Activities toward the Scientific Team." CEAS Space Journal, Vol. 10, No. 4, 2018, pp. 487–500. doi:10.1007/s12567-018-0205-9.

[7]Fichter, W., Gath, P., Vitale, S., and Bortoluzzi, D. "LISA Pathfinder Drag-Free Control and System Implications." Classical and Quantum Gravity, Vol. 22, No. 10, 2005. doi:10.1088/0264-9381/22/10/002.

[8]Dittus, H., Lammerzahl, C., and Turyshev, S. G. Lasers, Clocks and Drag-Free Control. 2008.

[9]Canuto, E. "Drag-Free and Attitude Control for the GOCE Satellite." Automatica, Vol. 44, No. 7, 2008, pp. 1766–1780. doi:10.1016/j.automatica.2007.11.023.

[10]Canuto, E., and Massotti, L. "All-Propulsion Design of the Drag-Free and Attitude Control of the European Satellite GOCE." Acta Astronautica, Vol. 64, 2009, pp. 325–344.

[11]Edwards, C. H., Wallace, N. C., Tato, C., and Van Put, P. "The T5 Ion Propulsion Assembly for Drag Compensation on GOCE." European Space Agency, (Special Publication) ESA SP, Vol. 2004, No. 569, 2004, pp. 217–223.

[12]Pettazzi, L., Lanzon, A., Theil, S., and Finzi, A. E. "Design of Robust Drag-Free Controllers with Given Structure." Journal of Guidance, Control, and Dynamics, Vol. 32, No. 5, 2009, pp. 1609–1621. doi:10.2514/1.40279.

[13]Yoon, H., Eun, Y., and Park, C. "Adaptive Tracking Control of Spacecraft Relative Motion with Mass and Thruster Uncertainties." Aerospace Science and Technology, Vol. 34, No. 1, 2014, pp. 75–83. doi:10.1016/j.ast.2014.02.002.

[14]Choueiri, E. Y. "Plasma Oscillations in Hall Thrusters." Physics of Plasmas, Vol. 8, No. 4, 2001, pp. 1411–1426. doi:10.1063/1.1354644.

[15]Wei, L. Q., Han, L., Yu, D. R., and Guo, N. "Low-Frequency Oscillations in Hall Thrusters." Chinese Physics B, Vol. 24, No. 5, 2015, pp. 1–10. doi:10.1088/1674-1056/24/5/055201.

[16]Liu, H., Chen, P. B., Sun, Q. Q., Hu, P., Meng, Y. C., Mao, W., and Yu, D. R. "Design of a Cusped Field Thruster for Drag-Free Flight." Acta Astronautica, Vol. 126, No. September, 2016, pp. 35–39. doi:10.1016/j.actaastro.2016.04.009.

[17]Cui, K., Liu, H., Jiang, W. J., Sun, Q. Q., Hu, P., and Yu, D. R. "Effects of Cusped Field Thruster on the Performance of Drag-Free Control System." Acta Astronautica, Vol. 144, No. October 2017, 2018, pp. 193–200. doi:10.1016/j.actaastro.2017.12.032.

[18]Keller, A. Feasibility of a Down-Scaled HEMP Thruster. Justus-Liebig-University Giessen, 2013.

[19]Gath, P., Fichter, W., Kersten, M., and Schleicher, A. Drag Free and Attitude Control System Design for the LISA Pathfinder Mission. 2004.

[20]Curtis, H. Orbital Mechanics for Engineering Students (Third Edition). Elsevier, 2014.

[21]NRLMSISE-00 Atmosphere Model. https://ccmc.gsfc.nasa.gov/modelweb/models/nrlmsise00.php. Accessed Mar. 28, 2018.

[22]Blandino, J. J., Marchetti, P., and Demetriou, M. A. "Electric Propulsion and Controller Design for Drag-Free Spacecraft Operation." Journal of Spacecraft and Rockets, Vol. 45, No. 6, 2008, pp. 1303–1315. doi:10.2514/1.36307.